Photosphere – Internal Shock Model of Gamma-Ray Bursts: Implications for the Fermi/LAT Results

(arXiv: 1002.2634; being revised)

Kenji Toma
with
Xue-Feng Wu & Peter Meszaros
(Penn State Univ)

Gamma-Ray Bursts 2010 Conference, Nov 1-4, 2010, Annapolis, MD

Outline

1. Prompt Emission: Observations and Models
2. Standard Fireball Model: Photospheric Emission
3. Ph-IS Model: Temporal Properties
4. Ph-IS Model: Spectral Properties
5. Case Studies: GRB 080916C, 090902B, 090510
6. Summary & Discussion

Prompt Emission: Observations

Before *Fermi*
- mainly observed in 10 keV – 1 MeV
- Band or CPL spectrum (Preece+00; Ghirlanda+02; Kaneko+06)
- variable light curve

Fermi observations (Fermi team papers 09;10)
- observed in 8 keV – 300 GeV

- Band spectrum in 10 keV – 10 GeV (GRB 080825C, 080916C, ...)
- Band + distinct PL (GRB 090510, 090902B, 090926A)

- delayed onset in > 100 MeV (due to the flux increase and/or spectral change)
- variable light curve in > 100 MeV (GRB 090510, 090926A)

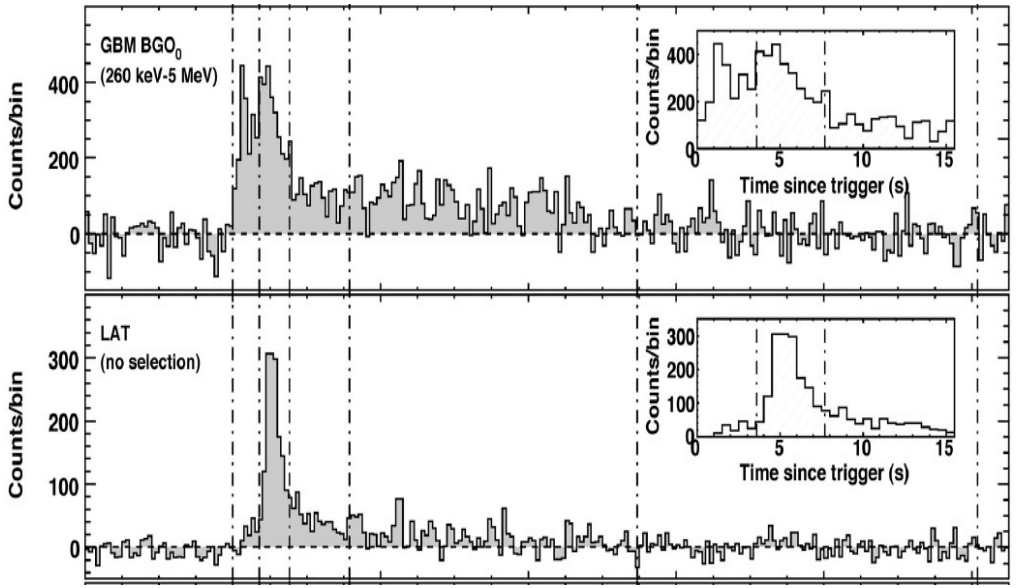

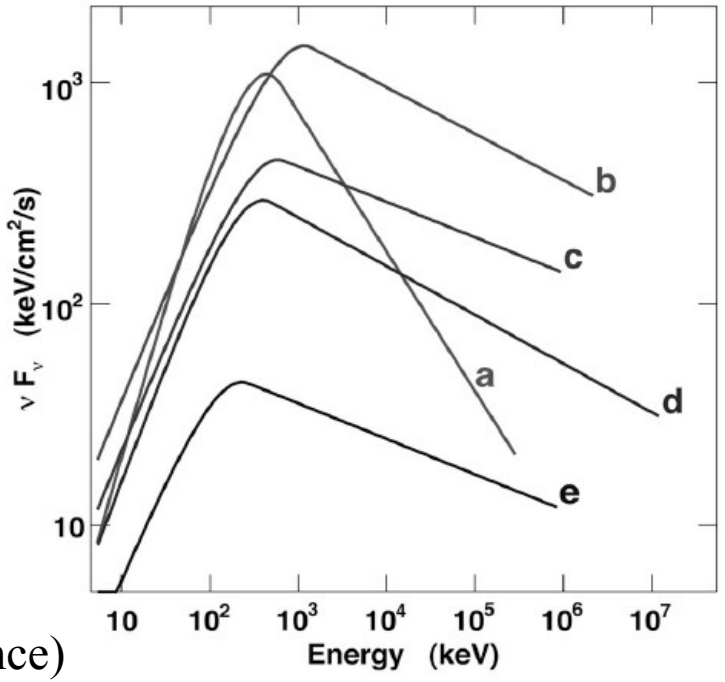

GRB 080916C
(Abdo+09, Science)

Prompt Emission: Models

Three types of models actively discussed for the Band component (<10MeV)
- Photospheric emission models (e.g. Paczynski 86; Thompson 94; Meszaros & Rees 00)
- Internal shock models (e.g. Rees & Meszaros 94; Kobayashi+ 97; Daigne & Mochkovitch 98)
- Magnetic dissipation models (e.g. Drenkhahn & Spruit 02; Lyutikov 06)

Clarifying the origin of the prompt emission would help understand the nature of the relativistic jets and the central compact objects.

Origin of the distinct components and the onset delays in the high-energy range (> 100 MeV) ?

- External shock models (Kumar & Barniol Duran 09; Ghisellini+10) → variability ?

- Internal shock models (Abdo+09; Corsi+09; Daigne+10) → SSC onset delay not larger than variability timescale
- Cocoon EIC model (Toma+09) needs $\epsilon_B \sim 10^{-5}$

- Hadronic emission models (Asano+09; Razzaque+10) need large energy budgets

- Magnetic dissipation models → ? (see Zhang10, Fan 10)

We focus on the photospheric emission models.

External shock emission is suggested to be insufficient (He+ 10; Liu & Wang 10)

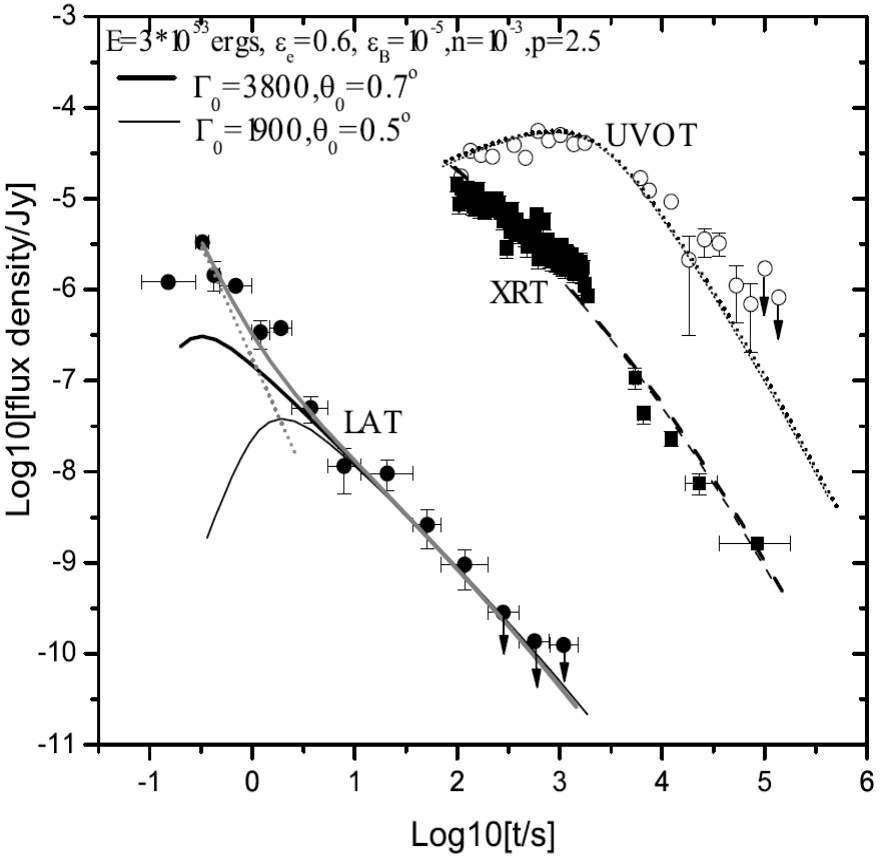

2. Photospheric Emission Models

The standard fireball model

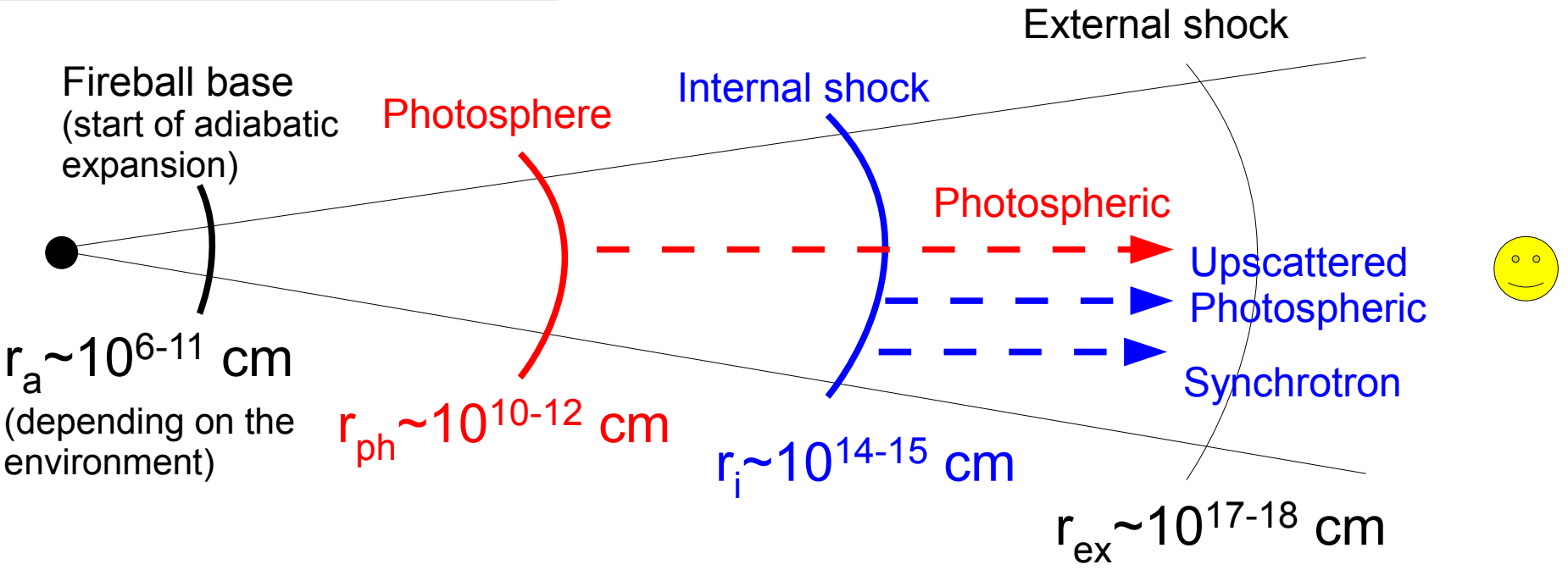

- The photospheric emission is naturally bright around ~ 1 MeV (Paczynski 86: Goodman 86)
- There could be some effects which cause a non-thermal dissipation of the jet at $r_a < r < r_{ph}$ and make a non-thermal tail of the photospheric emission.

These may be associated with copious pair creation (Rees & Meszaros 05; Pe'er+05; Ioka+07; Beloborodov 10; Lazzati & Begelman 10; Thompson 94)

- The high-energy emission may not be from the photosphere, but may be instead from a dissipation region out of the photosphere (Gao+09; Ryde+10)
- The UP emission is a good candidate for the high-energy emission (This work; Pe'er+10)

Photospheric Emission

Fireball dynamics:

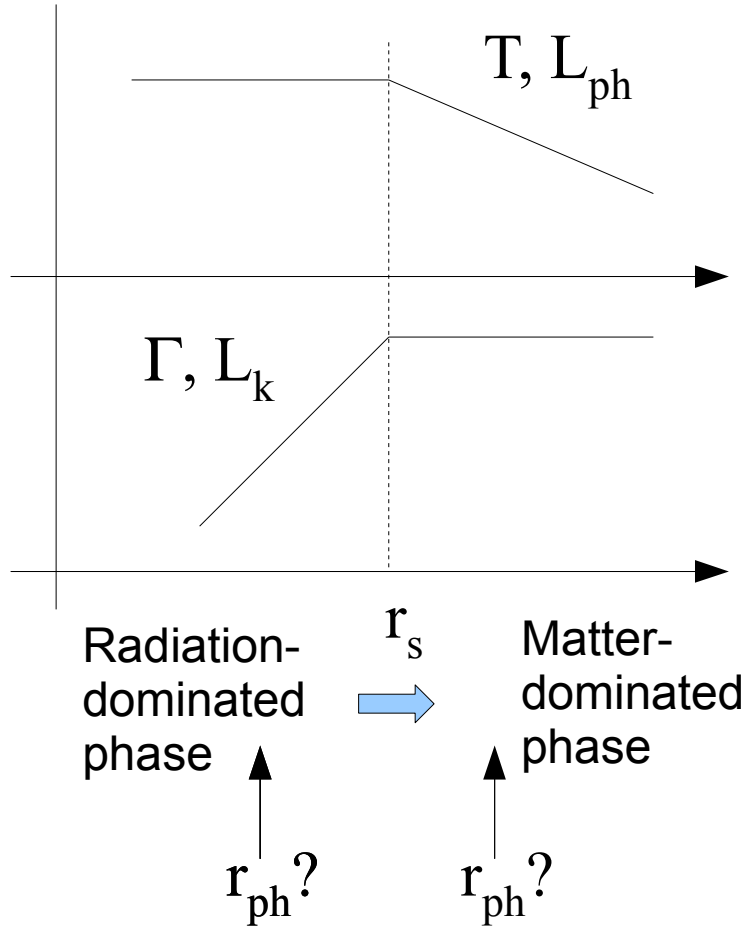

Key parameter: $\eta \equiv L/\dot{M}c^2,$

Critical value:

$$\eta_* = \left(\frac{\sigma_T \mathcal{R} L \Gamma_a}{8\pi r_a m_p c^3}\right)^{1/4} \simeq 2.8\times 10^3\, L_{53}^{1/4} \left(\frac{r_{a,7}}{\Gamma_a}\right)^{-1/4} \mathcal{R}_1^{1/4}.$$

$$n'_l = \mathcal{R} n',$$

Low baryon load case: $\eta > \eta_* \quad r_{\rm ph} < r_s$

$$L_{\rm ph} \approx L, \quad \varepsilon_{\rm ph} \simeq 4\, kT_a, \quad \Gamma_f \simeq \eta_*, \quad L_k \simeq L\left(\frac{\eta}{\eta_*}\right)^{-1}.$$

High baryon load case: $\eta < \eta_* \quad r_{\rm ph} > r_s$

$$L_{\rm ph} \simeq L\left(\frac{\eta}{\eta_*}\right)^{8/3}, \quad \varepsilon_{\rm ph} \simeq 4\, kT_a \left(\frac{\eta}{\eta_*}\right)^{8/3}$$

$$\Gamma_f = \eta, \quad L_k \approx L.$$

The observer-frame temperature at the base:

$$T_a = \left(\frac{L\Gamma_a^2}{4\pi r_a^2 ca}\right)^{1/4} \simeq 2\, L_{53}^{1/4} \left(\frac{r_{a,7}}{\Gamma_a}\right)^{-1/2} \ {\rm MeV}/k,$$

Photospheric emission can be dominant in the MeV energy range.

3. Ph-IS Model: Temporal Properties

Simple kinematic consideration:

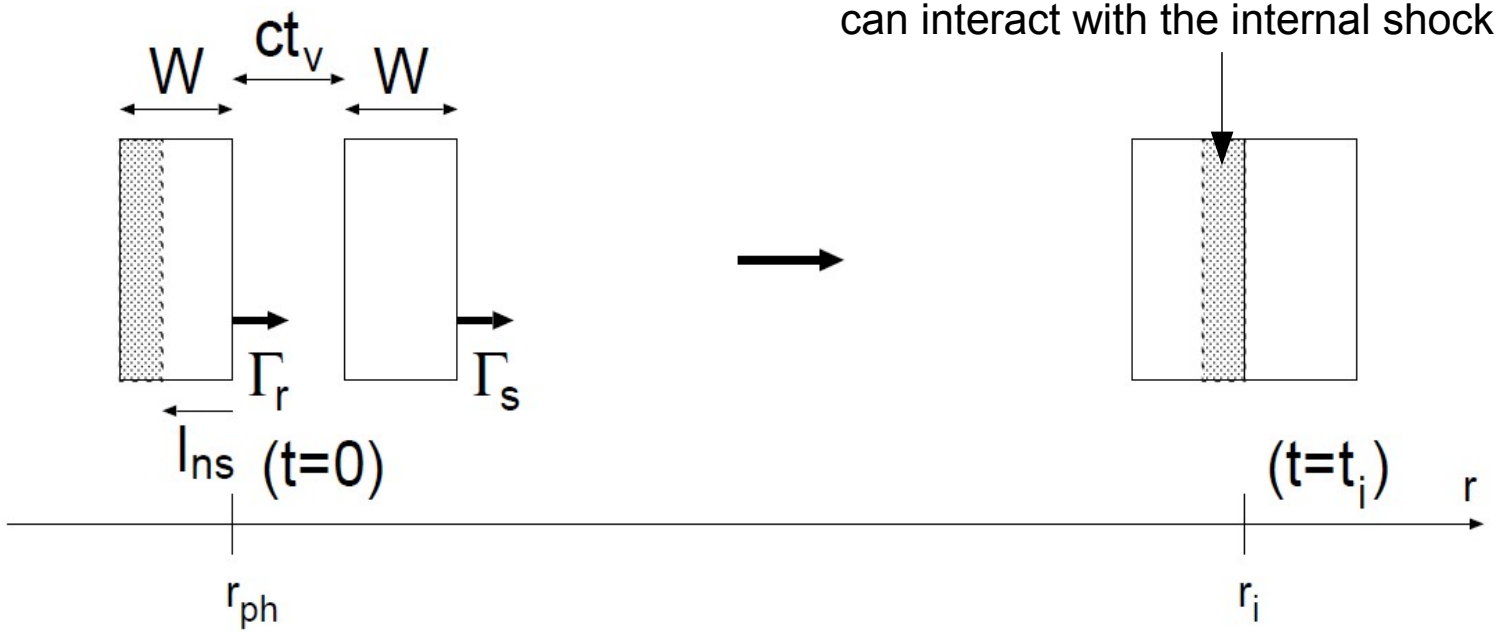

Photospheric photons (from the rapid shell) that can interact with the internal shock particles

$a_L = \eta_r/\eta_s \lesssim 5.$

$\epsilon_d \lesssim 0.25.$

$l_{\rm ns} = c(1-\beta_r)t_i \approx a_L^{-2} c t_v.$ $< W/2$: *efficient scattering regime*

(Typical case $W \sim c\, t_v$ is included)

Up-scattered photospheric (UP) emission pulses are correlated with the photospheric pulses from rapid shells, and lagged from the photospheric pulses from slow shells. $t_{\rm lag} = (W + ct_v + l_{\rm ns})/c \sim (W/c) + t_v.$

This lag is comparable to t_v or $\delta t_{\rm ph} \sim \frac{W}{c}$. The observed LAT onset delays are very large compared with the variability timescale. We will propose another explanation for the observed delays in the end of this talk.

4. Ph-IS Model: Spectral Properties (3 slides)

Internal shock radius:

$$r_i \simeq 2ct_v\eta_s^2 = 2ct_v\eta^2 a_L^{-2} \simeq 2\times 10^{13}\eta_3^2 t_{v,-2}(a_L/5)^{-2}\ \mathbf{cm}.$$

Minimum injection energy of accelerated leptons:

$$\gamma_m = \frac{m_p}{m_e}\frac{p-2}{p-1}\mathcal{R}^{-1}\epsilon_d\epsilon_e \simeq 4\,\mathcal{R}_1^{-1}\left(\frac{\epsilon_d\epsilon_e}{0.1}\right) f(p),$$

Magnetic field amplification:

$$U'_B = B'^2/(8\pi) = L\epsilon_d\epsilon_B/(4\pi r_i^2 c\eta^2).$$

Synchrotron, SSC, UP emission energy densities:

$$U'_{\rm syn} = t'_{\rm dyn}\frac{4}{3}\sigma_T c U'_B\int\gamma^2\frac{dn'_l}{d\gamma}d\gamma = xU'_B, \qquad U'_{\rm ssc} = xU'_{\rm syn}, \qquad U'_{\rm up} = xU'_{\rm ph},$$

$$\begin{cases} L_{\rm up} \simeq xL_{\rm ph}, \\ L_{\rm syn} \simeq \epsilon_d\epsilon_B xL \simeq kxL_{\rm ph}, \\ L_{\rm ssc} \simeq \epsilon_d\epsilon_B x^2 L \simeq kx^2 L_{\rm ph}, \end{cases}$$

$$x = \frac{4}{3}\sigma_T\frac{r_i}{2\eta}\int\gamma^2\frac{dn'_l}{d\gamma}d\gamma \simeq \frac{4(p-1)}{3(p-2)}\tau_{l,i}\gamma_m\gamma_c h(\gamma_m,\gamma_c),$$

$$k \equiv \frac{\epsilon_d\epsilon_B}{(\eta/\eta_*)^{8/3}}.$$

The cooling energy of leptons can be estimated by:

$$\gamma_c m_e c^2 = P(\gamma_c) r_i/(2c\eta) \qquad P(\gamma) = (4/3)\sigma_T c\gamma^2 (U'_B + U'_{\rm syn} + U'_{\rm ph})$$

Table 1. Ordering of emission luminosities for various cases of $\mathcal{G} = (\eta/\eta_*)^{8/3}$, $\mathcal{E} = \epsilon_d \epsilon_e h$, and $\mathcal{B} = \epsilon_d \epsilon_B$.

Case	$\mathcal{G}$	k(or k'), x		Luminosities	$\mathcal{E}$ and $\mathcal{B}$
1	$\eta < \eta_*(\mathcal{G} < 1)$	$k \ll 1,\ kx \ll 1$	$x \ll 1$	$L_{\rm ph} \gg L_{\rm up} \gg L_{\rm syn} \gg L_{\rm ssc}$	$\mathcal{G} \gg \max(\mathcal{E}, \mathcal{B})$
2			$x \gg 1,\ kx^2 \ll 1$	$L_{\rm up} \gg L_{\rm ph} \gg L_{\rm ssc} \gg L_{\rm syn}$	$\mathcal{E} \gg \mathcal{G} \gg (\mathcal{E}^2\mathcal{B})^{1/3} \gg \mathcal{B}$
3			$x \gg 1,\ kx^2 \gg 1$	$L_{\rm up} \gg L_{\rm ssc} \gg L_{\rm ph} \gg L_{\rm syn}$	$\mathcal{E} \gg (\mathcal{E}^2\mathcal{B})^{1/3} \gg \mathcal{G} \gg \mathcal{B}$
4		$k \ll 1,\ kx \gg 1$		$L_{\rm ssc} \gg L_{\rm up} \gg L_{\rm syn} \gg L_{\rm ph}$	$\mathcal{E} \gg (\mathcal{E}\mathcal{B})^{1/2} \gg \mathcal{G} \gg \mathcal{B}$
5		$k \gg 1$	$x \gg 1$	$L_{\rm ssc} \gg L_{\rm syn} \gg L_{\rm up} \gg L_{\rm ph}$	$\mathcal{E} \gg \mathcal{B} \gg \mathcal{G}$
6			$x \ll 1,\ kx \gg 1,\ kx^2 \gg 1$	$L_{\rm syn} \gg L_{\rm ssc} \gg L_{\rm ph} \gg L_{\rm up}$	$\mathcal{B} \gg \mathcal{E} \gg \mathcal{E}^2/\mathcal{B} \gg \mathcal{G}$
7			$x \ll 1,\ kx \gg 1,\ kx^2 \ll 1$	$L_{\rm syn} \gg L_{\rm ph} \gg L_{\rm ssc} \gg L_{\rm up}$	$\mathcal{B} \gg \mathcal{E} \gg \mathcal{G} \gg \mathcal{E}^2/\mathcal{B}$
8			$x \ll 1,\ kx \ll 1$	$L_{\rm ph} \gg L_{\rm syn} \gg L_{\rm up} \gg L_{\rm ssc}$	$\mathcal{B} \gg \mathcal{G} \gg \mathcal{E}$
9	$\eta > \eta_*(\mathcal{G} > 1)$	$k' \ll 1,\ k'x \ll 1$	$x \ll 1$	$L_{\rm ph} \gg L_{\rm up} \gg L_{\rm syn} \gg L_{\rm ssc}$	$\mathcal{G} \gg \max(\mathcal{E}, \mathcal{B})$

Cases 1, 2, 3, 9:

$$x \approx \frac{\epsilon_d \epsilon_e h}{(\eta/\eta_*)^{8/3}} \quad (k \ll 1, kx \ll 1).$$

Cases 4:

$$x \approx \sqrt{\epsilon_e h/\epsilon_B} \quad (k \ll 1, kx \gg 1).$$

Cases 5, 6, 7, 8:

$$x \approx \begin{cases} \sqrt{\epsilon_e h/\epsilon_B}, & (x \gg 1), \\ \epsilon_e h/\epsilon_B, & (x \ll 1). \end{cases} \quad (k \gg 1)$$

$\Rightarrow$ Consistent with model of synchrotron/SSC only (Sari & Esin 01)

$\mathcal{G} \equiv (\eta/\eta_*)^{8/3}$, $\mathcal{E} \equiv \epsilon_d \epsilon_e h$, and $\mathcal{B} \equiv \epsilon_d \epsilon_B$ divide spectral models into two: photospheric emission models and synchrotron/SSC emission models.

An example of case 1: $L_{53} = 3, \eta_3 = 3, r_{a,7}/\Gamma_a = 1, \mathcal{R}_1 = 2, \beta_{\rm ph} = -2.5,$

$t_{v,-2} = 1, p = 2.3, \epsilon_d\epsilon_e = 0.1, \epsilon_d\epsilon_B = 0.03,$ and $a_L = 5.$

$(\eta/\eta_*)^{8/3} \sim 0.4 > \max(\epsilon_d\epsilon_d h, \epsilon_d\epsilon_B),$ $r_{\rm ph} \sim 1 \times 10^{11}$ cm $r_i \sim 2\times10^{14}$ cm

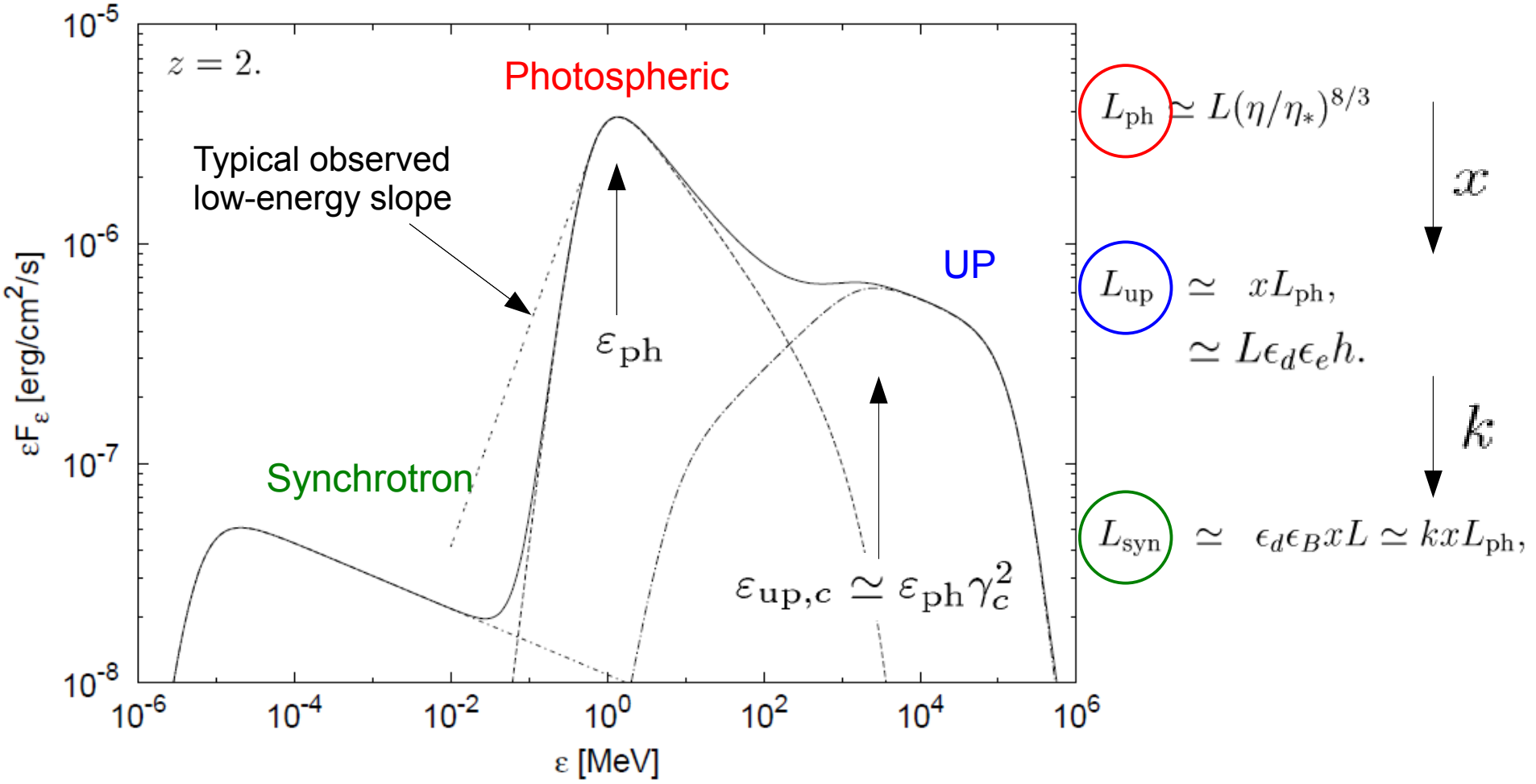

An approximate analytical form with smoothed breaks of each spectral component is used. Photospheric and UP components are dominant in the MeV and high-energy ranges, respectively.

Model Fit: GRB 080916C

Second time-bin:

$$L_{\rm up}/L_{\rm ph} = x \sim 0.2. \quad \epsilon_d\epsilon_e \lesssim 0.1$$

$$x \approx \frac{\epsilon_d\epsilon_e h}{(\eta/\eta_*)^{8/3}} \Rightarrow \eta < \eta_*$$

Seven model parameters
L, η, r_a/Γ_a, $\mathcal{R}$, $\epsilon_d\epsilon_e$, t_v, and a_L.
can be determined uniquely by
$L_{\rm ph}$, $\varepsilon_{\rm ph}$, $L_{\rm up}$, γ_c, and γ_m,
for reasonable values of
$\epsilon_d\epsilon_e \sim 0.1$ and $a_L \sim 5$,

First time-bin:

$$L_{\rm up}/L_{\rm ph} = x \lesssim 0.06. \Rightarrow \eta \gtrsim \eta_*$$

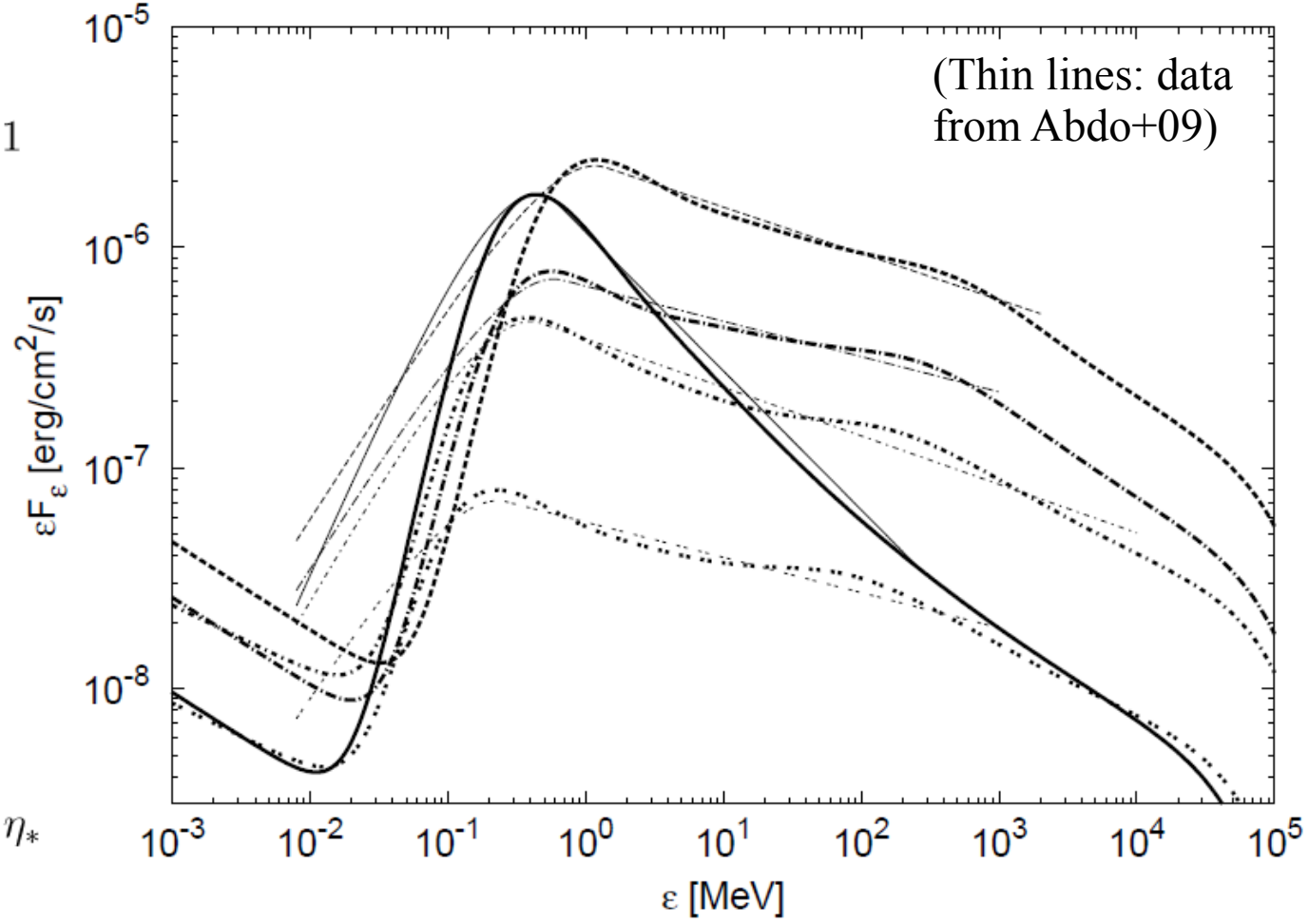

UP luminosity increase is due to the shift of the parameter regime; from $\eta > \eta_*$ into $\eta < \eta_*$

GRB 080916C[a]	Time-bin	L_{53}	$r_{a,7}/\Gamma_a$	η_3	$\mathcal{R}_1$	$\beta_{\rm ph}$	$t_{v,-2}$	p	$\epsilon_d\epsilon_e$	$\epsilon_d\epsilon_B$	η/η_*
	$0.0-3.6$ s	3	20	3.2	2	-3.0	0.3	2.8	0.1	<1	2
		3	20	3.1	2	-2.7	0.1	2.8	0.01	<1	2
	$3.6-7.7$ s	10	0.9	4.9	3	-2.5	0.2	2.8	0.1	$\lesssim 0.1$	0.7
	$7.7-15.8$ s	5	1	3.2	3	-2.5	0.6	2.8	0.1	$\lesssim 0.1$	0.6
	$15.8-54.7$ s	3	1	2.5	3	-2.5	0.7	2.6	0.1	$\lesssim 0.1$	0.5
	$54.7-100.8$ s	0.7	2	1.6	3	-2.5	1.5	2.6	0.1	$\lesssim 0.2$	0.5

Fine tuning not needed for Band-like shapes

The second time-bin spectrum of GRB 080916C

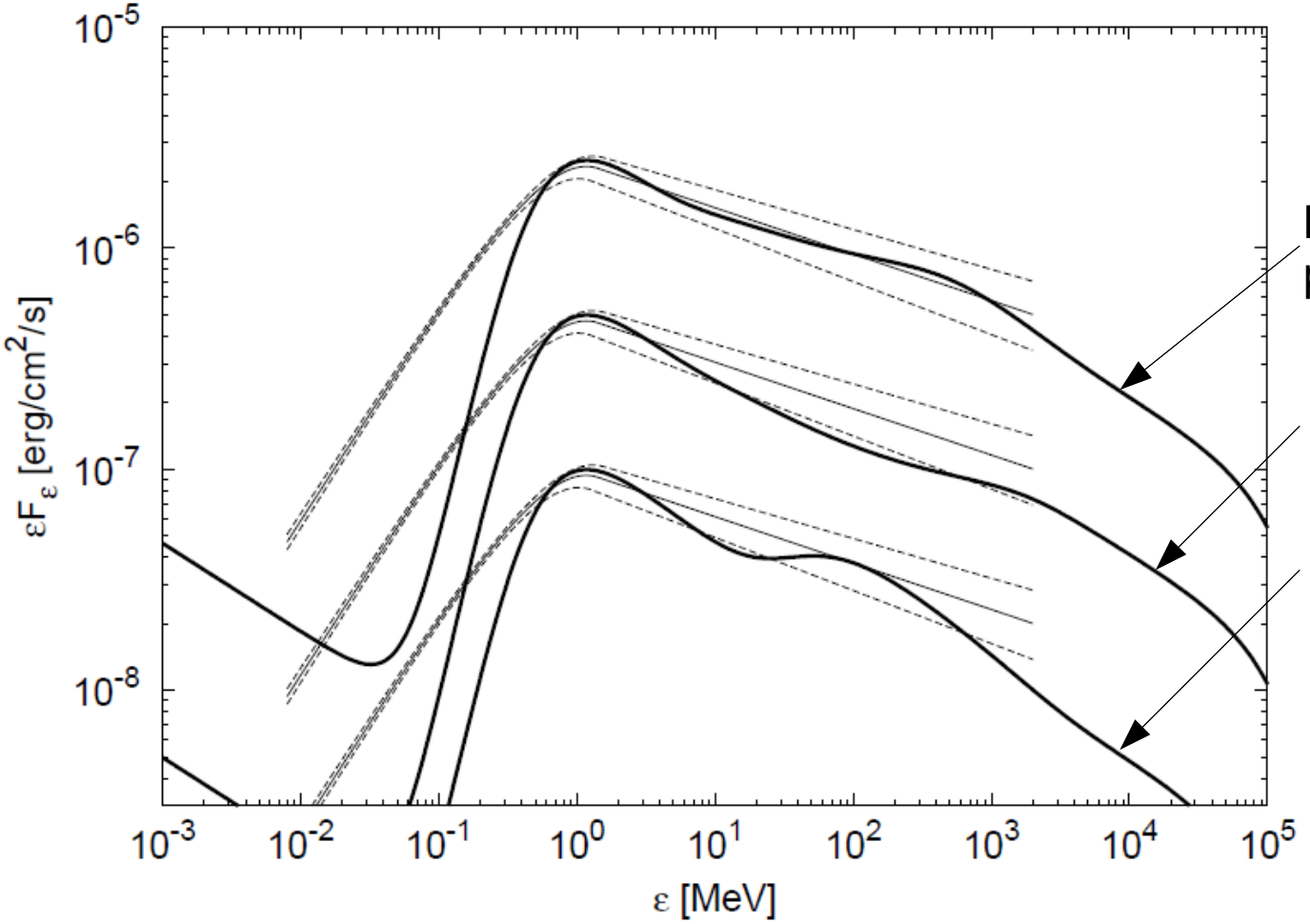

Best fit model parameters

$t'_v = 2t_v$, (Flux*0.2)

$\mathcal{R}' = \mathcal{R}/2$, (Flux*0.04)

The model spectra with t_v two times larger or R two times smaller than the best fit parameters seem to be still well fitted by a Band-like function, and consistent with the observed flux within a 1 sigma error.

Model Fit: GRB 090902B

Second time-bin:

$$L_{\rm up}/L_{\rm ph} = x \sim 0.05. \quad \epsilon_d\epsilon_e \lesssim 0.1$$

$$h = (\gamma_c/\gamma_m)^{2-p}/(3-p) \lesssim 0.3,$$

$$x \approx \frac{\epsilon_d\epsilon_e h}{(\eta/\eta_*)^{8/3}} \Rightarrow \eta < \eta_*$$

Best fit model parameters are similar to the second time-bin of GRB 080916C except for t_v and β_{ph}

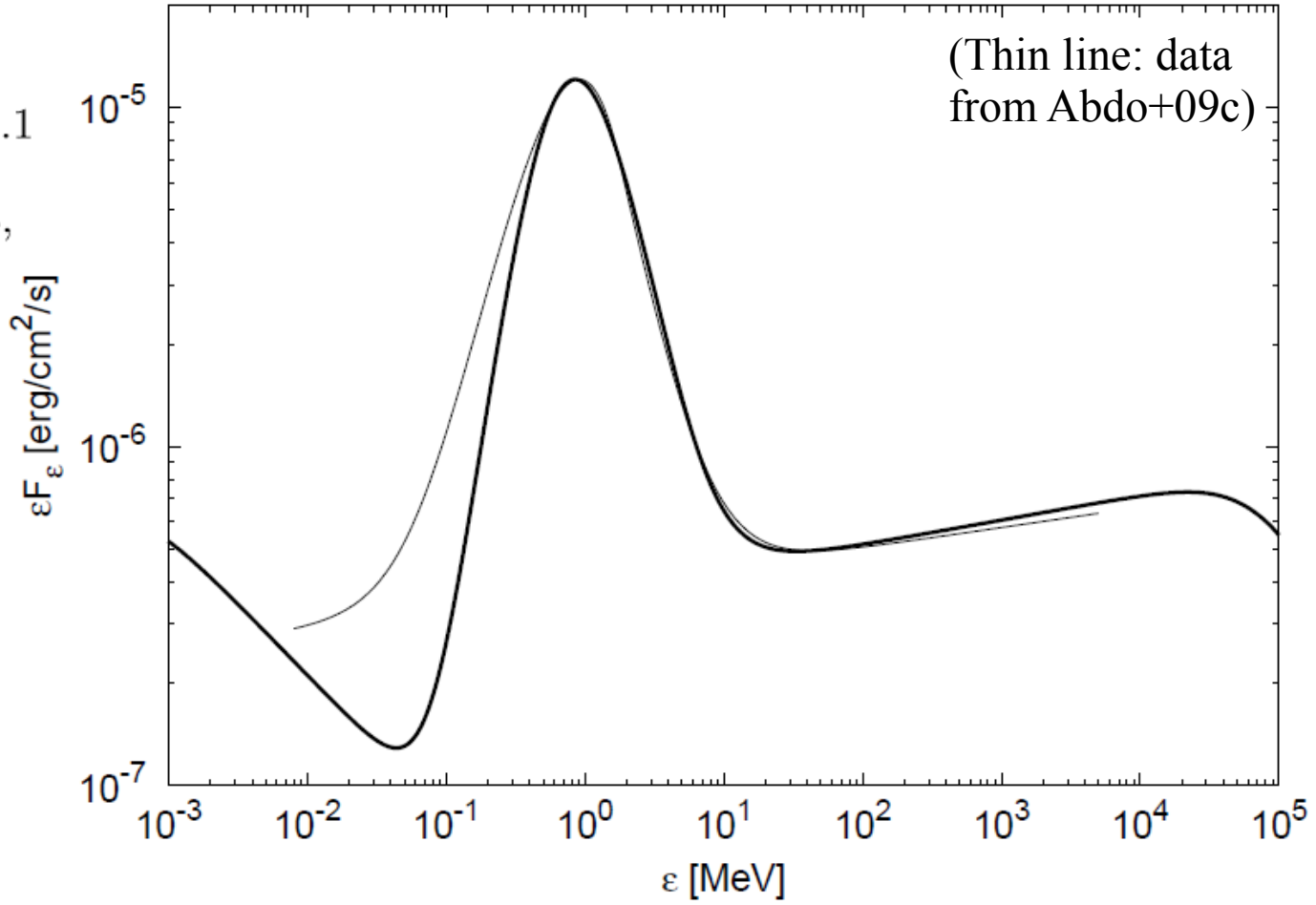

GRB 090902B	Time-bin	L_{53}	$r_{a,7}/\Gamma_a$	η_3	$\mathcal{R}_1$	$\beta_{\rm ph}$	$t_{v,-2}$	p	$\epsilon_d\epsilon_e$	$\epsilon_d\epsilon_B$	η/η_*
	$4.6-9.6$ s	12	2	3.3	3	-4.0	10	2.85	0.1	$\lesssim 0.2$	0.6

GRB 080916C[a]	Time-bin	L_{53}	$r_{a,7}/\Gamma_a$	η_3	$\mathcal{R}_1$	$\beta_{\rm ph}$	$t_{v,-2}$	p	$\epsilon_d\epsilon_e$	$\epsilon_d\epsilon_B$	η/η_*
	$0.0-3.6$ s	3	20	3.2	2	-3.0	0.3	2.8	0.1	<1	2
		3	20	3.1	2	-2.7	0.1	2.8	0.01	<1	2
	$3.6-7.7$ s	10	0.9	4.9	3	-2.5	0.2	2.8	0.1	$\lesssim 0.1$	0.7

Model Fit: GRB 090510

Second time-bin:

$$L_{\rm up}/L_{\rm ph} = x \sim 0.1, \qquad \epsilon_d\epsilon_e \lesssim 0.1$$

$$h \lesssim 0.7.$$

$$x \approx \frac{\epsilon_d\epsilon_e h}{(\eta/\eta_*)^{8/3}} \Rightarrow \eta < \eta_*$$

First time-bin:

$$L_{\rm up}/L_{\rm ph} = x \lesssim 3\times10^{-3}.$$

$$\Rightarrow \eta \gtrsim \eta_*$$

Third time-bin:

This spectrum is unique: $L_{up} > L_{ph}$

⇒ Case 2

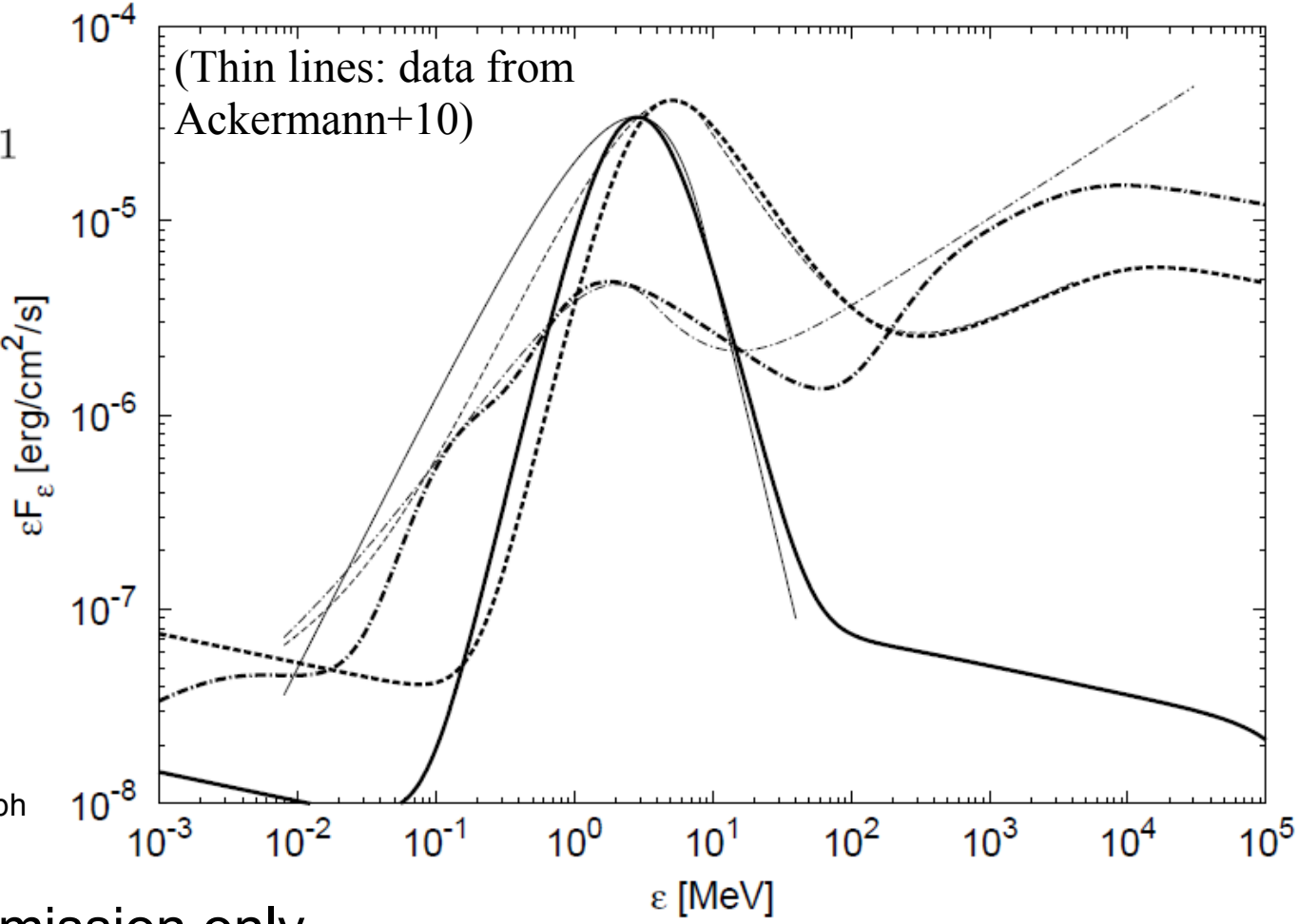

Fourth time-bin: the LAT emission only

Could be the high-latitude emission with a very large t_v

$$\delta t_{\rm up} \sim \frac{W}{c} + \frac{3r_i}{2c\Gamma_m^2} \simeq \frac{W}{c} + 3a_L^{-1}t_v.$$

GRB 090510	Time-bin	L_{53}	$r_{a,7}/\Gamma_a$	η_3	$\mathcal{R}_1$	$\beta_{\rm ph}$	$t_{v,-2}$	p	$\epsilon_d\epsilon_e$	$\epsilon_d\epsilon_B$	η/η_*
	$0.5-0.6$ s	1	3	73	2	-4.8	0.3	2.3	0.1	<1	30
		1	3	5.4	2	-4.8	0.1	2.3	5×10^{-3}	<1	2
	$0.6-0.8$ s	4	0.3	4.7	2	-3.0	0.2	2.3	0.1	$\lesssim 7\times10^{-3}$	0.7
	$0.8-0.9$ s	4	0.02	2.1	0.5	-2.5	0.7	2.25	0.15	$\lesssim 2\times10^{-4}$	0.3
		4	0.04	1.2	0.5	-2.5	20	2.25	0.15	$\lesssim 5\times10^{-4}$	0.2

Summary & Discussion (3 slides)

1. Radially inhomogeneous jets naturally produce variable photospheric emission around the MeV energy range, and can lead to internal shocks out of the photosphere. We have shown that the photospheric emission is efficiently up-scattered by the internal shocked electrons (and positrons).

2. We have derived various spectral types which depends on the values of $(\eta/\eta_*)^{8/3}$, $\epsilon_d\epsilon_e h$, and $\epsilon_d\epsilon_B$, and obtained necessary conditions for photospheric emission models.

$(\eta/\eta_*)^{8/3} \gg \max(\epsilon_d\epsilon_e h, \epsilon_d\epsilon_B)$ ⇒ Photospheric around MeV, UP in high-energy range

3. This case can be consistent with the time-binned spectra of LAT GRBs (as well as other GRBs observed at < 10 MeV). The low-energy spectrum of the photospheric emission is $\alpha_{ph} = 1$, which is much harder than observed, $\alpha_{ph} \sim -1$. The superposition of the emission from the multiple shells have the potential of reproducing the observed spectral slope.

4. Observed LAT onset delays larger than the variability timescales may not be explained as the simple kinematic effect but instead due to the shift of the parameter regime:

$\eta > \eta_*$ small $L_{\rm up}/L_{\rm ph} = x$ ⇒ $\eta < \eta_*$ large $L_{\rm up}/L_{\rm ph} = x$

The model fits of the data indicates that this shift is related to the decrease of r_a/Γ_a.

For GRB 080916C, r_a/Γ_a decreases from ~10^8cm to ~10^7cm. This may be consistent with a collapsar model, in which the front portion of the jet is expected to be strongly dissipated.

$r_a \sim 5 \times 10^{10}$ cm, $\Gamma_a \sim 500.$ ⇒ $r_a \sim 10^7$ cm, $\Gamma_a \sim 1.$

This may lead to a delay timescale r_a/c ~ 1 sec.

For GRB 090510, r_a/Γ_a decreases from ~$3*10^7$cm to ~$3*10^5$cm, suggesting a smaller size of the progenitor and the central object. This can be consistent with a smaller delay ~ 0.1sec.

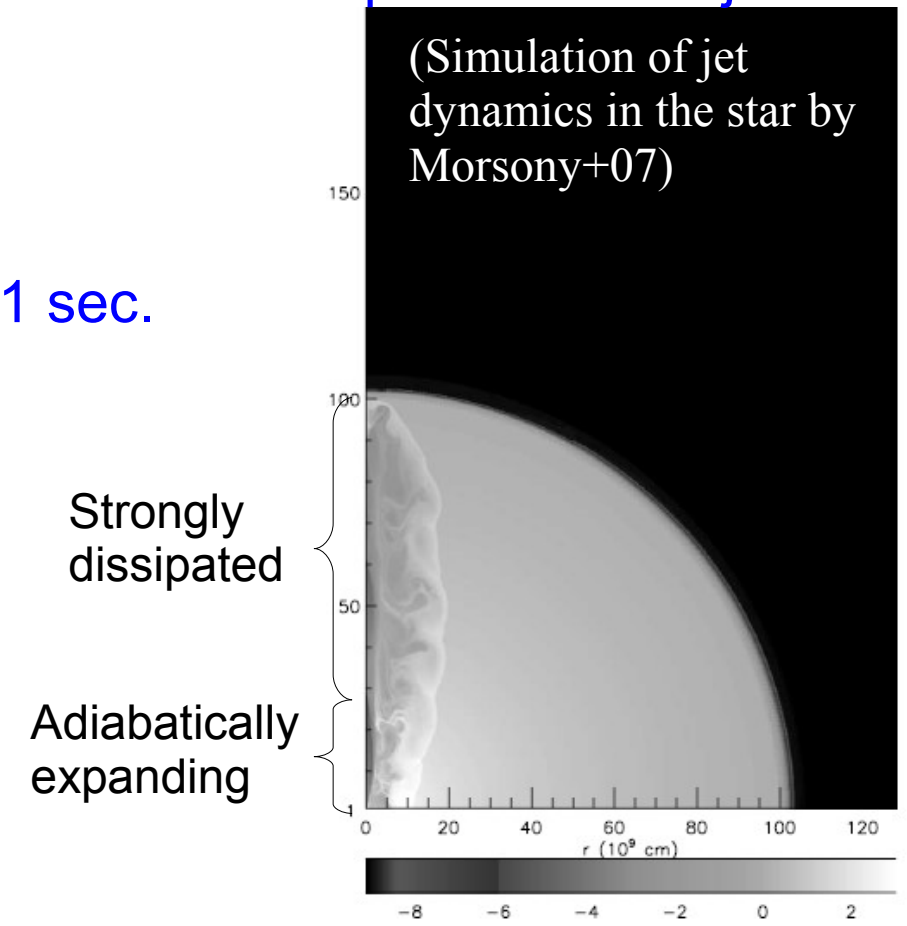

5. Rough calculations of the prompt emission efficiency, $\Sigma(L_{ph}+L_{up})t_{bin}/\Sigma Lt_{bin,}$ are ~30% for GRB 080916C, ~20% for GRB 090902B, and ~40% for GRB 090510. The standard external shock model of the late radio/opt/X afterglow of GRB 090902B indicates the efficiency ~80% (Cenko+10; see also Pe'er+10). This value can be reduced if only a fraction of the electrons are accelerated in the external shock (Eichler & Waxman 05; Toma+08).

6. The spectrum in the high-energy range may have spectral breaks at $\varepsilon_{up,h}$ and at ε_{KN}, while a break due to the electron-positron pair creation in the emission site is estimated to be typically much above those breaks in our model. Detecting spectral breaks in the high-energy range by Fermi/LAT (<100GeV) and/or by the future CTA (>30GeV) would be very helpful to constrain the models.

Low-energy spectral slope

An outstanding problem in the photospheric emission models, as well as in the synchrotron/SSC models is that the low-energy spectrum of the Band component. The Rayleigh-Jeans slope α_{ph}=1 is much harder than observed slope α~-1. The superposition of the photospheric emissions from multiple shells with different peak energies has the potential of reproducing the low-energy spectrum.

$$L_{\rm ph} \simeq L \left(\frac{\eta}{\eta_*}\right)^{8/3}, \quad \varepsilon_{\rm ph} \simeq 4\, kT_a \left(\frac{\eta}{\eta_*}\right)^{8/3}$$

$$\Rightarrow \quad L_{\rm ph} \propto \varepsilon_{\rm ph}$$

with different η and similar L, r_a/Γ_a, and $\mathcal{R}$

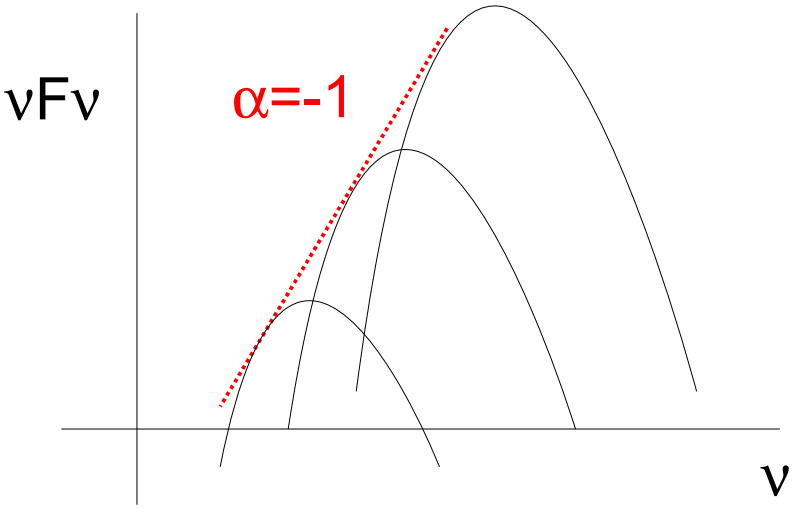

This is just a speculation, and we need more detailed consistency checks.

Our model fits indicate that t_v ~ 0.1s for GRB 090902B and t_v ~ 0.001s for GRB 080916C. This might be consistent with the report by Zhang B.B.+10 that the spectrum of GRB 090902B is more like blackbody for smaller time-bin, while the spectrum of GRB 080916C keeps highly non-thermal for smaller time-bin (>~1s).

Yonetoku relation in a burst

The spectral peak of the Band components of the time-binned spectra obeys the so-called Yonetoku relation.

$$\varepsilon_{\rm ph} \propto L_{\rm ph}^{1/2}$$

This may be a problem for all the emission models.

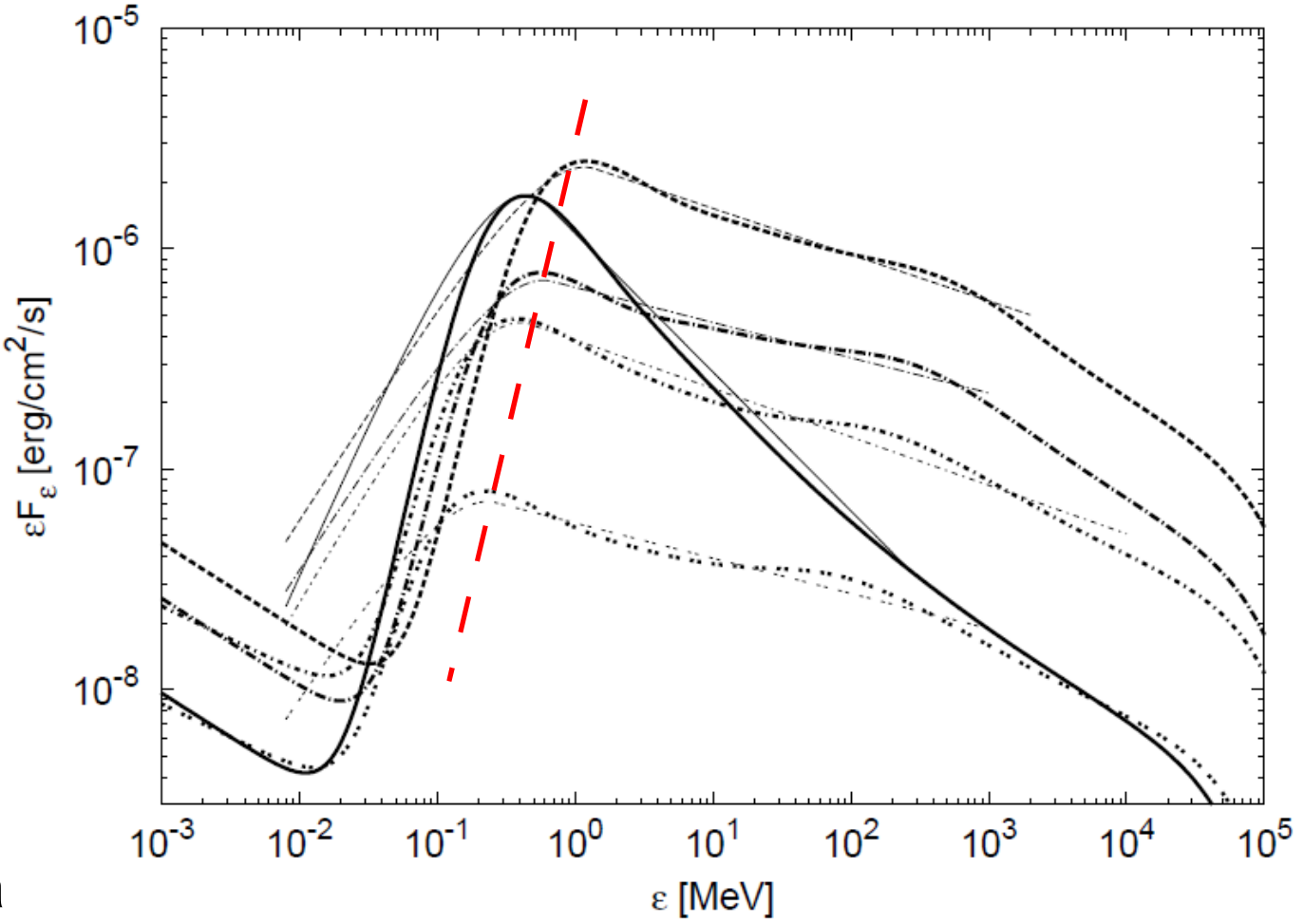

In our type of the photospheric emission model, this data require a relation between the physical parameters

$$L_{\rm ph} \simeq L\left(\frac{\eta}{\eta_*}\right)^{8/3}, \quad \varepsilon_{\rm ph} \simeq 4\,kT_a\left(\frac{\eta}{\eta_*}\right)^{8/3} \Rightarrow \quad \eta \propto L^{7/16}(r_a/\Gamma_a)^{1/8}\mathcal{R}^{1/4}$$